



Brazilian Journal of Physics

ISSN: 0103-9733

luizno.bjp@gmail.com

Sociedade Brasileira de Física

Brasil

Matheus, R. D.; Navarra, F. S.; Nielsen, M.

Rise and fall of pentaquarks in the QCD Sum Rules approach

Brazilian Journal of Physics, vol. 36, núm. 4b, diciembre, 2006, pp. 1397-1409

Sociedade Brasileira de Física

São Paulo, Brasil

Available in: <http://www.redalyc.org/articulo.oa?id=46413543014>

- How to cite
- Complete issue
- More information about this article
- Journal's homepage in redalyc.org

redalyc.org

Scientific Information System

Network of Scientific Journals from Latin America, the Caribbean, Spain and Portugal

Non-profit academic project, developed under the open access initiative

## Rise and Fall of Pentaquarks in the QCD Sum Rules Approach

R. D. Matheus, F. S. Navarra, and M. Nielsen

*Instituto de Física, Universidade de São Paulo, C.P. 66318, 05315-970 São Paulo, SP, Brazil*

Received on 18 March, 2006

We review the existing mass and decay width determinations of pentaquarks with QCD Sum Rules (QCDSR). We give special attention to the intermediate assumptions and choices which we are obliged to do in this approach. As an example, we present the full calculation of the pentaquark mass with Borel sum rules and also with Finite Energy Sum Rules (FESR). We also work out the calculation of the  $\Theta$  decay width. We take the opportunity to comment our publications on this subject and include new and unpublished material.

Keywords: Mass and decay; Pentaquarks; QCD Sum Rules

### I. INTRODUCTION

From June 2003 to August 2005 there was an intense theoretical activity devoted to understand the structure of a new family of baryons: the pentaquarks. The interest for this subject was triggered by the announcement made by the LEPs collaboration [1] reporting the observation of the  $\Theta^+(1540)$ . Since then, a flurry of theoretical [2] and experimental [3] papers brought the pentaquarks to the main stage of hadron physics.

The subsequent experimental searches, carried out in dozens of different machines with different energies, different beam and targets and different detection methods turned out to be inconclusive, half of the experiments observing the  $\Theta^+(1540)$  and the other half not observing it. This puzzling situation began to change when, in the beginning of 2005 some groups which had previously found the pentaquark state could not see it anymore in a second round of much more careful experiments [4, 5]. Very fast the community started not to believe in the existence of the pentaquark. In August 2005, a statement made by Ted Barnes at the HADRON05 meeting, in Rio de Janeiro, reflected this new consensus [6]. He said: “the pentaquark is dead!”. Much experimental work on the subject is still needed, not only to confirm the negative result, but also to understand what was wrong before. In spite of some isolated claims that the state really exists, today it seems very likely that the final conclusion will give support to the “death sentence” pronounced by Barnes. As for explaining the previous positive results, some steps along this direction have been taken by Meier, Dzierba and Szczepaniak, who tried to demonstrate that the signal observed by the CLAS collaboration at JLAB is a consequence, among other things, of kinematical reflections [7].

On the theoretical side the situation became equally confusing. The method able to give the best answers, lattice QCD, was used by several groups to look for the pentaquark [8–10]. These “theoretical searches”, in the same way as the initial experimental ones, turned out to be inconclusive, half of the groups finding a signal and half not finding it. Quark models were also extensively used in this context but they may give answer to different questions. Due to their very nature, they have to assume that a particle exists and then they may predict, for example, its spatial and color configuration.

Between lattice QCD and quark models, in an intermedi-

ate position in the theoretical scenario, we have QCD sum rules (QCDSR) [11–13], which, in principle are pure theory. However, due to the option of keeping the calculation analytic and avoiding the “brute force” numerical work; due to the option of trading a simulation of the QCD vacuum by the phenomenological parameters known as condensates, the results start to depend on certain assumptions (like, for example, the factorization hypothesis for higher dimension condensates) which are made during the calculations. The first works on  $\Theta^+(1540)$  with QCDSR [14–17] addressed the mass of the state and could all obtain a reasonable value for the mass. Later, a more careful analysis [18–20] revealed some problems with the previous calculations. In the mean time other pentaquarks were observed: the  $\Xi^{--}$  and the  $\Theta_c$ . These were also studied with QCDSR [18, 21]. This time, with more rigorous criteria it was more difficult to reproduce the experimental data, i.e., the masses of the states (especially the  $\Xi^{--}$ ). Finally, attempts to describe the extremely narrow decay width pushed the method to the limit and the conclusion was that it is very difficult to understand this decay in QCDSR [22].

If, in the near future, the non-existence of pentaquarks is confirmed, the community might address to the QCDSR practitioners the following justified and embarrassing question: “how could you so nicely calculate the correct mass of something that does not exist?”

In this work we present a critical review of these QCDSR calculations commenting their strong and weak points. In reviewing these topics we present new material, which was never published before.

The text is organized as follows. In the next section we briefly mention some interesting facts and main ideas about pentaquarks. In section 3 we present the main formulas of QCDSR, show one complete calculation of a pentaquark mass with all the inputs and assumptions. In section 4 we enumerate the requirements that must be satisfied for a QCDSR calculation to be reliable and check whether this is the case for the results discussed in the preceding section. In section 5 we introduce the finite energy sum rules (FESR) and present the results for  $m_\Theta$  and  $m_\Xi$  obtained with this method. In section 6 we move to the pentaquark decay width. Finally, in section 7 we present our conclusions.

## II. THE PENTAQUARK STRUCTURE

Probably the most interesting physical question related to pentaquarks is: how are these five quarks organized? The exotic baryon with the  $K^+n$  quantum numbers, the  $\Theta^+(1540)$ , first observed in [1], could not be a three quark state and its minimal quark content had to be  $uudd\bar{s}$ . These quarks could be in one of the following configurations: a) uncorrelated quarks inside a bag [23]; b) a  $K-N$  molecule bound by a van-der Waals force [24]; c) a “ $K-N$ ” bound state in which  $uud$  and  $u\bar{s}$  are not separately in color singlet states [14]; d) a diquark-triquark  $(ud) - (ud\bar{s})$  bound state [25] and e) a diquark-diquark-antiquark state [26]. This last possibility has been by far the most explored, also in the QCD sum rules framework.

According to Jaffe and Wilczek (JW), each diquark should have spin zero and should be in the  $\bar{\mathbf{3}}$  representation of  $SU(3)$ , in color and flavor. The two diquark would then combine in a  $P$ -wave orbital angular momentum to form a  $\mathbf{3}$  state in color, spin  $S = 0$ , and  $\bar{\mathbf{6}}$  in flavor. The resulting state would then be combined with the antiquark to form a flavor antidecuplet  $\mathbf{10}_f$  and octet  $\mathbf{8}_f$ , with spin  $S = 1/2$ . The  $\Theta^+$  would be at the top of the antidecuplet  $\mathbf{10}_f$  and would have an isospin  $I = 0$ . JW have also interpreted the lightest particle in the octet  $\mathbf{8}_f$ ,  $[ud]^2\bar{d}$ , as the Roper resonance, since it has the same quantum numbers of the nucleon. The Roper resonance would be thus identical to the  $\Theta^+$  except for the substitution of the strange antiquark by a down antiquark. This would explain why the mass difference between  $\Theta^+(1540)$  and  $N(1440)$  is so close to the strange quark mass.

Understanding the organization of matter at the quark level is of extreme importance. This can be done with the help of lattice QCD and, to some extent, with QCDSR. In the following section we describe the calculation of a pentaquark mass with QCDSR.

## III. CORRELATION FUNCTION, CURRENTS AND MASSES

The purpose of this section is mainly to show the QCDSR machinery at work, giving emphasis to the aspects which may be potential sources of uncertainties.

In the QCDSR approach [12, 13], the short range perturbative QCD is extended by an operator product expansion (OPE) of the correlators, which results in a series in powers of the squared momentum with Wilson coefficients. The convergence at low momentum is improved by using a Borel transform. The expansion involves universal quark and gluon condensates. The quark-based calculation of a given correlator is equated to the same correlator, calculated using hadronic degrees of freedom via a dispersion relation, providing sum rules from which a hadronic quantity can be estimated. The QCDSR calculation of hadronic masses centers around the two-point correlation function given by

$$\Pi(q) \equiv i \int d^4x e^{iq \cdot x} \langle 0 | T \eta(x) \bar{\eta}(0) | 0 \rangle \quad (1)$$

where  $\eta(x)$  is an interpolating field (a current) with the quantum numbers of the hadron we want to study.

In the next subsections we discuss the evaluation of (1) for the cases of the  $\Xi^{--}$  and of the  $\Theta^+$ .

The basic ingredients in the particle mass determinations from QCD spectral sum rules [11, 12] as well as from lattice QCD calculations are the interpolating currents used to describe the particle states. Contrary to the ordinary mesons, where the form of the current is unique, there are different choices of the pentaquark currents in the literature. We shall list below some possible operators describing the isoscalar  $I = 0$  and  $J = 1/2$  channel which would correspond to the experimental candidate  $\Theta(1540)$ .

### A. The $\Theta(1540)$ currents

Defining the pseudoscalar ( $ps$ ) and scalar ( $s$ ) diquark interpolating fields as:

$$\begin{aligned} Q_{ab}^{ps}(x) &= [u_a^T(x) C d_b(x)] , \\ Q_{ab}^s(x) &= [u_a^T(x) C \gamma_5 d_b(x)] , \end{aligned} \quad (2)$$

where  $a, b, c$  are color indices and  $C$  denotes the charge conjugation matrix, the lowest dimension current built by two diquarks and one anti-quark describing the  $\Theta$  as a  $I = 0, J^P = 1/2^+$   $S$ -wave resonance is [16]:

$$\eta_I^\Theta = \epsilon^{abc} \epsilon^{def} \epsilon^{cfg} Q_{ab}^{ps} Q_{de}^s C \bar{s}_g^T, \quad (3)$$

and the one with one diquark and three quarks is [14]:

$$\eta_{III}^\Theta = \frac{1}{\sqrt{2}} \epsilon^{abc} Q_{ab}^s \{ u_e \bar{s}_e i \gamma_5 d_c - (u \leftrightarrow d) \}. \quad (4)$$

This later choice can be interesting if the instanton repulsive force arguments [27] against the existence of a pseudoscalar diquark bound state apply. Alternatively, a description of the  $\Theta$  as a  $I = 0, J^P = 1/2^+$   $P$ -wave resonance has been proposed by [26] and used by [17] in the sum rule analysis:

$$\eta_{III}^\Theta = \left( \epsilon^{abd} \delta^{ce} + \epsilon^{abc} \delta^{de} \right) [Q_{ab}^s (D^\mu Q_{cd}^s) - (D^\mu Q_{ab}^s) Q_{cd}^s] \gamma_5 \gamma_\mu C \bar{s}_e^T. \quad (5)$$

This current can be generalized by considering its mixing with the following one having the same dimension and quantum numbers:

$$\eta_{IV}^\Theta = \epsilon^{abc} \epsilon^{def} \epsilon^{cfg} Q_{ab}^{ps} Q_{de}^s \gamma_\mu (D^\mu C \bar{s}_g^T). \quad (6)$$

The evaluation of (1) with (6) revealed that [19], to leading order in  $\alpha_s$  and in the chiral limit  $m_q \rightarrow 0$ , the contribution to the correlator vanishes. This result justifies a posteriori the *unique choice* of operator for the  $P$ -wave state used in [17].

### B. The $\Xi(1862)$ currents

Following the diquark-diquark-antiquark scheme, we can write two independent interpolating fields with the quantum

numbers of  $\Xi^{--}$  ( $I = 3/2$ ,  $J^P = 1/2^-$ ):

$$\eta_1(x) = \frac{1}{\sqrt{2}} \epsilon_{abc} (d_a^T(x) C \gamma_5 s_b(x)) [d_c^T(x) C \gamma_5 s_e(x) + s_e^T(x) C \gamma_5 d_c(x)] C \bar{u}_e^T(x) \quad (7)$$

$$\eta_2(x) = \frac{1}{\sqrt{2}} \epsilon_{abc} (d_a^T(x) C s_b(x)) [d_c^T(x) C s_e(x) + s_e^T(x) C d_c(x)] C \bar{u}_e^T(x) \quad (8)$$

where  $a, b, c$  and  $e$  are color indices and  $C = -C^T$  is the charge conjugation operator.

As in the nucleon case, where one also has two independent currents with the nucleon quantum numbers [28, 29], the most general current for  $\Xi^{--}$  is a linear combination of the currents given above:

$$\eta_I^\Xi(x) = [t\eta_1(x) + \eta_2(x)], \quad (9)$$

with  $t$  being an arbitrary parameter. In the case of the nucleon, the interpolating field with  $t = -1$  is known as Ioffe's current [28]. With this choice for  $t$ , this current maximizes the overlap with the nucleon as compared with the excited states, and minimizes the contribution of higher dimension condensates. In the present case it is not clear a priori which is the best choice for  $t$ .

We also employ the following interpolating field operator for the pentaquark  $\Xi^{--}$  [10, 16]:

$$\eta_{II}^\Xi(x) = \epsilon^{abc} \epsilon^{def} \epsilon^{cfs} s_a^T(x) C d_b(x) \times s_d^T(x) C \gamma_5 d_e(x) C \bar{u}_g^T(x) \quad (10)$$

It is easy to confirm that this operator produces a baryon with  $J = 1/2$ ,  $I = 3/2$  and strangeness  $-2$ . The parts,  $S^c(x) = \epsilon^{abc} s_a^T(x) C \gamma_5 d_b(x)$  and  $P^c(x) = \epsilon^{abc} s_a^T(x) C d_b(x)$ , give the scalar  $S$  ( $0^+$ ) and the pseudoscalar  $P$  ( $0^-$ )  $sd$  diquarks, respectively. They both belong to the anti-triplet representation of the color SU(3). The scalar diquark corresponds to the  $I = 1/2$   $sd$  diquark with zero angular momentum. It is known that a gluon exchange force as well as the instanton mediated force commonly used in the quark model spectroscopy give significant attraction between the quarks in this channel.

### C. The $\Xi$ mass

Inserting Eq. (9) into the integrand of Eq. (1) we obtain

$$\begin{aligned} \langle 0 | T \eta(x) \bar{\eta}(0) | 0 \rangle &= t^2 \Pi_{11}(x) + t \Pi_{12}(x) \\ &+ t \Pi_{21}(x) + \Pi_{22}(x) \end{aligned} \quad (11)$$

Calling  $\Gamma_1 = \gamma_5$  and  $\Gamma_2 = 1$  we get

$$\begin{aligned} \Pi_{ij}(x) &= \langle 0 | T \eta_i(x) \bar{\eta}_j(0) | 0 \rangle \\ &= \epsilon_{abc} \epsilon_{a'b'c'} C S_{e'e}^T(-x) C \\ &\quad \{ -\text{Tr} [\Gamma_i S_{bb'}^s(x) \Gamma_j C S_{aa'}^T(x) C] \\ &\quad \times \text{Tr} [\Gamma_i S_{ee'}^s(x) \Gamma_j C S_{cc'}^T(x) C] + \dots \end{aligned} \quad (12)$$

where  $S_{ab}(x)$  and  $S_{ab}^s(x)$  are the light and strange quark propagators respectively. The above expression was included just to show the ingredients of the calculation. The full version of (12) can be found in [18].

In order to evaluate the correlation function  $\Pi(q)$  at the quark level, we first need to determine the quark propagator in the presence of quark and gluon condensates. Keeping track of the terms linear in the quark mass and taking into account quark and gluon condensates, we get [30]

$$\begin{aligned} S_{ab}(x) &= \langle 0 | T [q_a(x) \bar{q}_b(0)] | 0 \rangle \\ &= \frac{i\delta_{ab}}{2\pi^2 x^4} k - \frac{m_q \delta_{ab}}{4\pi^2 x^2} \\ &\quad - \frac{i}{32\pi^2 x^2} t_{ab}^A g_s G_{\mu\nu}^A (k \sigma^{\mu\nu} + \sigma^{\mu\nu} k) \\ &\quad - \frac{\delta_{ab}}{12} \langle \bar{q}q \rangle \\ &\quad - \frac{m_q}{32\pi^2} t_{ab}^A g_s G_{\mu\nu}^A \sigma^{\mu\nu} \ln(-x^2) \\ &\quad + \frac{i\delta_{ab}}{48} m_q \langle \bar{q}q \rangle k - \frac{x^2 \delta_{ab}}{2^6 \times 3} \langle g_s \bar{q} \sigma \cdot G q \rangle \\ &\quad + \frac{ix^2 \delta_{ab}}{2^7 \times 3^2} m_q \langle g_s \bar{q} \sigma \cdot G q \rangle k \\ &\quad - \frac{x^4 \delta_{ab}}{2^{10} \times 3^3} \langle \bar{q}q \rangle \langle g_s^2 G^2 \rangle \end{aligned} \quad (13)$$

where we have used the factorization approximation for the multi-quark condensates, and we have used the fixed-point gauge [30].

Inserting (13) into (12) we obtain a set of diagrams which contribute to the OPE side of the correlation function.

Lorentz covariance, parity and time reversal imply that the two-point correlation function in Eq. (1) has the form

$$\Pi(q) = \Pi_1(q^2) + \Pi_q(q^2) \not{q} \quad (14)$$

A sum rule for each scalar invariant function  $\Pi_1$  and  $\Pi_q$ , can be obtained. In [18] the chirality even structure  $\Pi_q(q^2)$  was used to obtain the final results.

The phenomenological side is described, as usual, as a sum of pole and continuum, the latter being approximated by the OPE spectral density. In order to suppress the condensates of higher dimension and at the same time reduce the influence of higher resonances we perform a standard Borel transform [12]:

$$\Pi(M^2) \equiv \lim_{n, Q^2 \rightarrow \infty} \frac{1}{n!} (Q^2)^{n+1} \left( -\frac{d}{dQ^2} \right)^n \Pi(Q^2) \quad (15)$$

( $Q^2 = -q^2$ ) with the squared Borel mass scale  $M^2 = Q^2/n$  kept fixed in the limit.

For current II we repeat the steps mentioned above, substituting (10) into (1), making use of the expansion (13), picking up the terms multiplying the structure  $\not{q}$  and finally performing a Borel transform (15).

After Borel transforming each side of  $\Pi_q(Q^2)$  and transferring the continuum contribution to the OPE side we obtain the

following sum rule at order  $m_s$ :

$$\lambda_{\Xi}^2 e^{-\frac{m_{\Xi}^2}{M^2}} = \int_0^{s_0} e^{-\frac{s}{M^2}} \rho_i^q(s) ds. \quad (16)$$

where  $i(=I, II)$  refers to the current employed and the spectral densities, up to order 6 are given by:

$$\begin{aligned} \rho_I^q(s) = & c_1 \frac{s^5}{5!5!2^{12}7\pi^8} + c_3 \frac{s^3}{5!2^{10}\pi^6} m_s \langle \bar{s}s \rangle \\ & - c_4 \frac{s^3}{5!2^8\pi^6} m_s \langle \bar{q}q \rangle + c_2 \frac{s^3}{5!3!2^{13}\pi^6} \langle \frac{\alpha_s}{\pi} G^2 \rangle \\ & + 7c_4 \frac{s^2}{2!6\pi^6} m_s \langle \bar{q}g_s \sigma \cdot \mathbf{G} q \rangle \\ & + c_2 \frac{s^2}{3!2^{11}\pi^4} (\langle \bar{s}s \rangle^2 + \langle \bar{q}q \rangle^2) \\ & + c_4 \frac{s^2}{3!2^8\pi^4} \langle \bar{s}s \rangle \langle \bar{q}q \rangle \\ & - c_5 \frac{s^2}{4!3!2^{11}\pi^6} m_s \langle \bar{s}g_s \sigma \cdot \mathbf{G} s \rangle \\ & - 3c_4 \frac{s^2}{4!3!2^{12}\pi^6} m_s \langle \bar{q}g_s \sigma \cdot \mathbf{G} q \rangle \\ & \times \left( 6 \ln\left(\frac{s}{\Lambda_{QCD}^2}\right) - \frac{43}{2} \right), \end{aligned} \quad (17)$$

with  $c_1 = 5t^2 + 2t + 5$ ,  $c_2 = (1-t)^2$ ,  $c_3 = (t+1)^2$ ,  $c_4 = t^2 - 1$ ,  $c_5 = t^2 + 22t + 1$ ,  $\Lambda_{QCD} = 110$  MeV and

$$\begin{aligned} \rho_{II}^q(s) = & \frac{s^5}{5!5!2^{10}7\pi^8} + \frac{s^3}{5!3!2^7\pi^6} m_s \langle \bar{s}s \rangle \\ & + \frac{s^3}{5!3!2^{10}\pi^6} \langle \frac{\alpha_s}{\pi} G^2 \rangle \\ & + \frac{s^2}{4!3!2^9\pi^6} m_s \langle \bar{s}g_s \sigma \cdot \mathbf{G} s \rangle. \end{aligned} \quad (18)$$

To extract the  $\Xi^{--}$  mass,  $m_{\Xi}$ , we take the derivative of Eq. (16) with respect to  $M^{-2}$  and divide it by Eq. (16). Repeating the same steps leading to (16), (17) and (18) for the chirality odd structure  $\Pi_1(q^2)$  we arrive at

$$\lambda_{\Xi}^2 m_{\Xi} e^{-\frac{m_{\Xi}^2}{M^2}} = \int_0^{s_0} e^{-\frac{s}{M^2}} \rho_i^1(s) ds. \quad (19)$$

where

$$\begin{aligned} \rho_I^1(s) = & -c_1 \frac{s^4}{5!4!2^{10}\pi^6} \langle \bar{q}q \rangle \\ & + c_1 \frac{s^3}{4!3!2^{12}\pi^6} \langle \bar{q}g_s \sigma \cdot \mathbf{G} q \rangle \end{aligned} \quad (20)$$

and

$$\begin{aligned} \rho_{II}^1(s) = & -\frac{s^4}{5!4!2^7\pi^6} \langle \bar{q}q \rangle \\ & + \frac{s^3}{4!3!2^9\pi^6} \langle \bar{q}g_s \sigma \cdot \mathbf{G} q \rangle \end{aligned} \quad (21)$$

In the numerical analysis of the sum rules, the values used for the condensates are:  $\langle \bar{q}q \rangle = -(0.23)^3 \text{ GeV}^3$ ,  $\langle \bar{s}s \rangle = 0.8 \langle \bar{q}q \rangle$ ,  $\langle \bar{s}g_s \sigma \cdot \mathbf{G} s \rangle = m_0^2 \langle \bar{s}s \rangle$  with  $m_0^2 = 0.8 \text{ GeV}^2$  and  $\langle g_s^2 G^2 \rangle = 0.5 \text{ GeV}^4$ . The gluon condensate has a large error of about a factor 2, but its influence on the analysis is relatively small. We define the continuum threshold as:

$$s_0 = (1.86 + \Delta)^2 \text{ GeV}^2 \quad (22)$$

In the complete theory, the mass extracted from the sum rule should be independent of the Borel mass  $M^2$ . However, in a truncated treatment there will always be some dependence left. Therefore, one has to work in a region where the approximations made are acceptable and where the result depends only moderately on the Borel variables.

A comparison between results obtained with different currents is more meaningful when they describe the same physical state, i.e., those with the same quantum numbers. Concerning spin, all currents considered in our work have the same spin ( $= 1/2$ ). Concerning the parity, the situation is more complicated. In QCD sum rules, when we construct the current, it has a definite parity. Current (9) has parity  $P = -1$  and current (10) has parity  $P = +1$ . However, currents can couple to physical states of different parities. As well discussed in [21], in order to know the parity of the state in QCDSR, we have to analyze the chiral-odd sum rule. If the r.h.s of this sum rule (containing the spectral density coming from QCD) is positive, then the parity of the corresponding physical state is the same as the parity of the current. If it is negative the parity is the opposite of the parity of the current. Performing this analysis we might determine in both cases the parity of the state. However it turns out that for both currents, in the chiral-odd sum rule the OPE does not have good convergence, i.e., terms containing higher order operators are not suppressed with respect to the lowest order ones. This sum rule is thus ill defined and nothing can be said about the parity of the state. The comparative study of the currents is still valid because we can compare other properties of these currents. A possible outcome of this study might be that one current has defects, which are so severe that we are forced to abandon it. If this turns out to be case, the determination of the parity of the associated states becomes irrelevant.

#### IV. RELIABILITY OF A QCD SUM RULE CALCULATION

Having presented the main formulas in the last section, the next step is to introduce numerical values for the masses and condensates, choose reasonable values for the free (or partially constrained) parameters, which are the continuum threshold, the Borel mass at which the mass sum rule is evaluated and, in the case of current (9), the value of  $t$ . As a result we obtain values for  $m_{\Xi}$ . In doing these calculations we must remember that *it is not enough to obtain a pentaquark mass consistent with the experimental number*. There is a list of requirements that must be fulfilled:

i) the physical observables, such as masses and coupling constants, must be approximately independent of the Borel mass (this is the so called Borel stability).

- ii) the right hand side (RHS) of the sum rules (16) and (19) must be positive, since the left hand side (LHS) is manifestly positive.
- iii) the operator product expansion (OPE) must be convergent, i.e., the terms appearing in (17) and (18) must decrease with the increasing order of the operator.
- iv) the pole contribution must be dominant, i.e., the integral in (16) and in (19) must be at least 50 % of the integral over the complete domain of invariant masses ( $s_0 \rightarrow \infty$ ).
- v) the threshold parameter  $s_0$  must be compatible with the energy corresponding to the first excitation of an usual baryon.

#### A. current (9)

After an extensive search for best values of parameters and optimal Borel window, we have realized that it is extremely difficult to satisfy simultaneously the conditions i)-v) given above. In particular, when we have a very good OPE convergence, the strength of the pole is very weak and vice versa. We have to look for a compromise.

In order to illustrate these results, we consider  $m_s = 0.10$  GeV and  $\Delta = 0.44$  GeV, and construct, Figs. 1, 2 and 3, showing the Borel mass dependence of  $m_{\Xi}$ , of the OPE terms (in absolute value) and of the percentage of the pole contribution respectively. For these choices the value of the current-state overlap is:

$$\lambda_I^q \simeq 5.4 \times 10^{-9} \text{ GeV}^{13} \quad (23)$$

Restricting ourselves to the parameter combinations which satisfy the requirements i) - v) and taking the average we obtain:

$$m_{\Xi} = 1.85 \pm 0.05 \text{ GeV} \quad (24)$$

We have also used a current composed by scalar diquarks only, i.e.,  $\eta_1$ . The motivation for studying this current is to verify if it gives a smaller mass for the pentaquark than those obtained with other currents. According to the instanton description of diquark dynamics, this should be the case. We observe that, for same choices for  $m_s$  and  $\Delta$ , the masses found with scalar diquark currents are only slightly smaller than the others. This means either that instanton dynamics was not captured by our choice of currents and diagrams or that the interaction between the pseudoscalar diquarks (included in the mixed currents) is more attractive than expected.

#### B. current (10)

Using the same numerical inputs quoted in the last subsection we evaluate now the sum rules obtained with current(10). The same comments made in the previous subsection apply here. Choosing  $m_s = 0.10$  GeV and  $\Delta = 0.24$  GeV, we present in Figs. 4, 5 and 6 the Borel mass dependence of  $m_{\Xi}$ , of the OPE terms and of the percentage of the pole respectively. As it

can be seen, with current(10) we tend to overestimate  $m_{\Xi}$ , unless very low threshold parameters or quark masses are used. Besides, the pole contribution is always smaller than 40 %. On the other hand, the Borel stability seen in Fig. 4 is remarkable. This suggests that we could choose a lower value for the Borel mass, thereby increasing the pole contribution without significantly changing  $m_{\Xi}$ . The average over the best parameter choices leads to:

$$m_{\Xi} = 1.88 \pm 0.04 \text{ GeV} \quad (25)$$

Finally, for these parameters the current-state overlap is:

$$\lambda_{II}^q \simeq 1.3 \times 10^{-9} \text{ GeV}^{13} \quad (26)$$

Comparing (23) and (26) we observe that the coupling of current I to the  $\Xi$  state is four times larger than the coupling of current II to this state. This speaks in favor of current I.

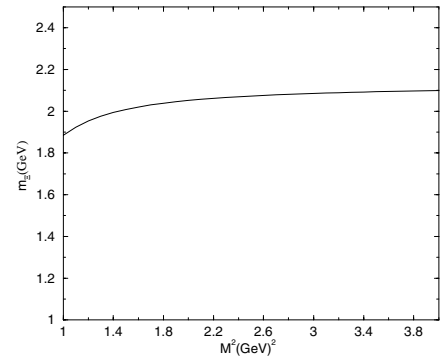


FIG. 1:  $\Xi$  mass with current I.  $m_s = 0.10$  GeV,  $t = 1$  and  $\Delta = 0.44$  GeV.

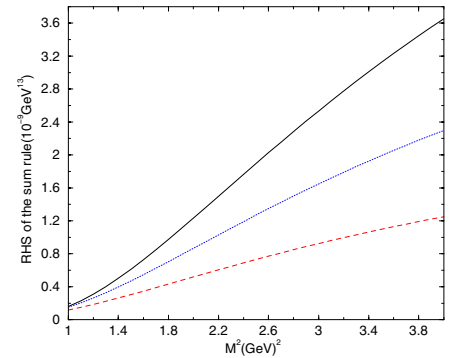


FIG. 2: Leading terms of the R.H.S. of (16) with current I.  $m_s = 0.10$  GeV,  $t = 1$  and  $\Delta = 0.44$  GeV. Solid line: perturbative term; dotted line: operators of dimension 4; dashed line: operators of dimension 6.

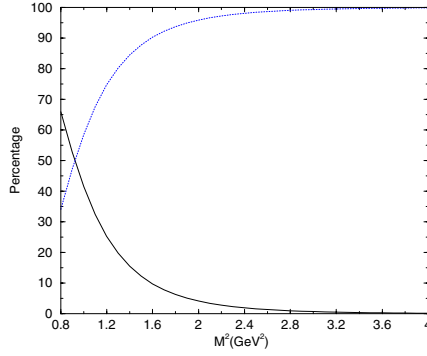


FIG. 3: Relative strength of the pole (solid line) and the continuum (dotted line) as a function of the Borel mass squared with current I.  $m_s = 0.10 \text{ GeV}$ ,  $t = 1$  and  $\Delta = 0.44 \text{ GeV}$ .

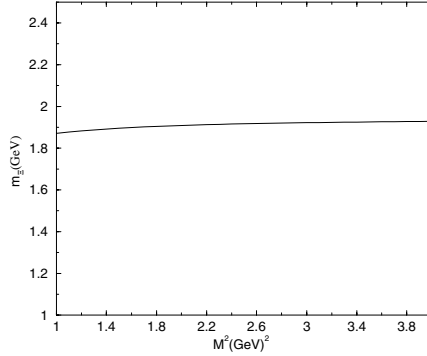


FIG. 4:  $\Xi$  mass with current II.  $m_s = 0.10 \text{ GeV}$  and  $\Delta = 0.24 \text{ GeV}$ .

## V. FINITE ENERGY SUM RULES

As we have seen, the description of the phenomenological side of the sum rules requires the definition of the spectral density  $\rho$ , which is written as a sum of pole and continuum contribution. The energy gap separating the ground state from the first excited state ( $\Delta$ ) or, equivalently, the squared mass of the first excitation,  $s_0$ , when not previously known from experiment, must be guessed. This can be considered as a weak point in the Borel sum rules. A way to reduce this arbitrariness is to work in the large Borel mass limit and try to completely determine  $s_0$ . This variant of QCDSR is called Finite Energy Sum Rules (FESR) [11, 32, 33].

We start from the general form taken by the QCDSR for any two point correlator:

$$\lambda^2 e^{-\frac{m^2}{M^2}} = \int_0^{s_0} e^{-\frac{s}{M^2}} \rho(s) ds. \quad (27)$$

Taking the limit  $\frac{1}{M^2} \rightarrow 0$  we get:

$$\sum_n (-m)^{2n} \lambda^2 \left( \frac{1}{M^2} \right)^n = \sum_n \int_0^{s_0} (-s)^n \left( \frac{1}{M^2} \right)^n \rho(s) ds. \quad (28)$$

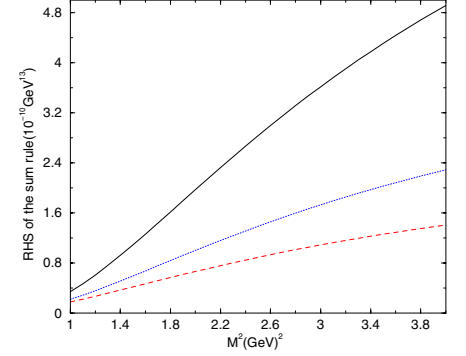


FIG. 5: Leading terms of the R.H.S of (16) with current II.  $m_s = 0.10 \text{ GeV}$  and  $\Delta = 0.24 \text{ GeV}$ . Solid line: perturbative term; dotted line: operators of dimension 4; dashed line: operators of dimension 6.

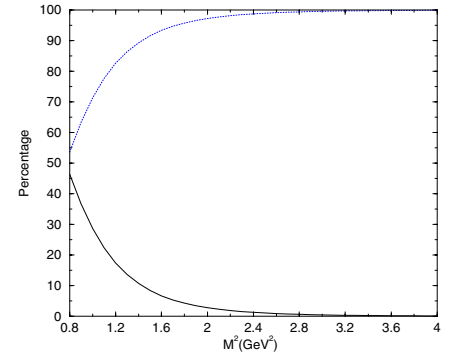


FIG. 6: Relative strength of the pole (solid line) and the continuum (dotted line) as a function of the Borel mass squared with current II.  $m_s = 0.10 \text{ GeV}$ ,  $t = 1$  and  $\Delta = 0.24 \text{ GeV}$ .

Equating the coefficients of the polynomial in  $\frac{1}{M^2}$  we get simply:

$$m^{2n} \lambda^2 = \int_0^{s_0} s^n \rho(s) ds, \quad n = 0, 1, 2, \dots \quad (29)$$

The mass can be easily obtained by dividing two of such equations with subsequent values of  $n$ :

$$m^2 = \frac{\int_0^{s_0} s^{n+1} \rho(s) ds}{\int_0^{s_0} s^n \rho(s) ds}, \quad n = 0, 1, 2, \dots \quad (30)$$

In contrast to the method discussed in the previous sections, the FESR have the advantage of giving correlations between the mass (and also  $\lambda$ ) and the QCD continuum threshold  $s_0$ , avoiding inconsistencies in the values of these parameters. Ideally, we can find a stability in the function  $m(s_0)$  thus having a good criterion for fixing both  $s_0$  and  $m$ .

On the other side, making  $\frac{1}{M^2} \rightarrow 0$  takes the sum rule to a region (high  $M^2$ ) where the pole contribution is almost zero (which can be seen quite clearly in figure 7).

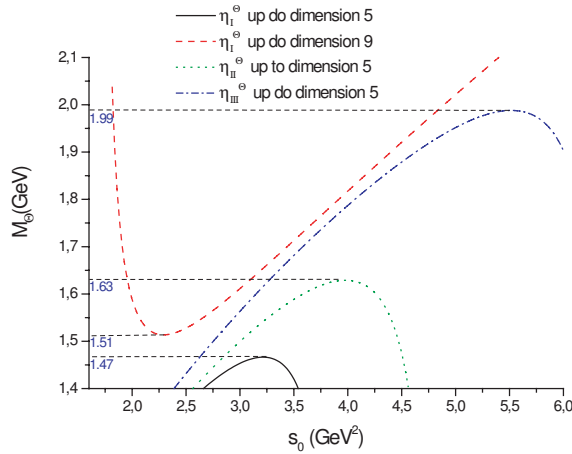


FIG. 7:  $m_\Theta$  obtained with the FESR for various currents up to dimension 5 condensates and up to dimension 9 in the case of  $\eta_I^\Theta$ . The values at the stability regions are indicated on the left.

#### A. The $\Theta^+$ (1540) mass

We proceed by applying the FESR to the currents in Eqs. (3), (4) and (5). This has been done fully for  $\eta_I^\Theta$  and  $\eta_{III}^\Theta$  in [19]. So we are going to omit the analytical expressions for these and concentrate in the FESR for  $\eta_{II}^\Theta$ , which are new. The FESR results for all three currents are presented here for the sake of comparison.

Performing the FESR analysis for the  $\Pi_q(q^2)$  structure, we notice that, at the approximation where the OPE is known (dimension  $\leq 6$ ), we do not have stability in  $s_0$  for any of the currents. Therefore, we used the  $\Pi_1(q^2)$  structure for the FESR.

To get the FESR for current (4) we start with the OPE expansion given in [14] and make  $\frac{1}{M^2} \rightarrow 0$ . We get:

$$\begin{aligned} \int_0^{s_0} \rho_I(s) ds &= \frac{m_s s_0^6}{1415577600\pi^8} - \frac{\langle \bar{s}s \rangle s_0^5}{29491200\pi^6} \\ &- \frac{7\langle \bar{q}q \rangle s_0^5}{14745600\pi^6} + \frac{\langle \bar{s}g\sigma Gs \rangle s_0^4}{4718592\pi^6} \\ &+ \frac{7\langle \bar{q}g\sigma Gq \rangle s_0^4}{2359296\pi^6} \end{aligned} \quad (31)$$

$$\begin{aligned} \int_0^{s_0} s\rho_{II}(s) ds &= \frac{m_s s_0^7}{1651507200\pi^8} - \frac{\langle \bar{s}s \rangle s_0^6}{35389440\pi^6} \\ &- \frac{7\langle \bar{q}q \rangle s_0^6}{17694720\pi^6} + \frac{\langle \bar{s}g\sigma Gs \rangle s_0^5}{5898240\pi^6} \\ &+ \frac{7\langle \bar{q}g\sigma Gq \rangle s_0^5}{2949120\pi^6} \end{aligned} \quad (32)$$

The mass is obtained dividing eq. (32) by eq.(31). The results are shown on figure 7 together with the results for currents (3) and (5) [19].

We can see in figure 7 that  $\eta_I^\Theta$  has the best agreement with the experimental candidate mass. The result from  $\eta_{II}^\Theta$  is a little high but still compatible with the experiments. The mass obtained with  $\eta_{III}^\Theta$  is so high that we are led to think that this current couples to an angular excitation [19]. This interpretation is reinforced by the derivatives in eq.(5). We should also note that  $\eta_I^\Theta$  stabilizes for very low values of  $s_0$ , especially when calculated in dimension 9, case in which  $\Delta s_0$  is very close to zero.

Summing up the results we have (the errors have been estimated for  $\eta_I^\Theta$  and  $\eta_{III}^\Theta$  in [19], here we assume an error of the same magnitude for  $\eta_{II}^\Theta$ ):

$$m_I^\Theta = (1.51 \pm 0.11)\text{GeV} \quad (33)$$

$$m_{II}^\Theta = (1.63 \pm 0.16)\text{GeV} \quad (34)$$

$$m_{III}^\Theta = (1.99 \pm 0.19)\text{GeV} \quad (35)$$

#### B. The $\Xi^{--}$ (1862) mass

In this subsection we repeat the steps above using the currents given by Eq.(9) and Eq.(10). As before, we have stability only in the structure  $\Pi_1(q^2)$ . For  $\eta_I^\Xi$  we obtain:

$$\int_0^{s_0} \rho_I(s) ds = -\frac{c_1 \langle \bar{q}q \rangle s_0^5}{14745600\pi^6} + \frac{c_1 \langle \bar{q}g\sigma Gq \rangle s_0^4}{2359296\pi^6}. \quad (36)$$

$$\int_0^{s_0} s\rho_I(s) ds = -\frac{c_1 \langle \bar{q}q \rangle s_0^6}{17694720\pi^6} + \frac{c_1 \langle \bar{q}g\sigma Gq \rangle s_0^5}{2949120\pi^6}, \quad (37)$$

where  $c_1 = 5t^2 + 2t + 5$ . For  $\eta_{II}^\Xi$ :

$$\int_0^{s_0} \rho_{II}(s) ds = -\frac{\langle \bar{q}q \rangle s_0^5}{1843200\pi^6} + \frac{\langle \bar{q}g\sigma Gq \rangle s_0^4}{294912\pi^6} \quad (38)$$

$$\int_0^{s_0} s\rho_{II}(s) ds = -\frac{\langle \bar{q}q \rangle s_0^6}{2211840\pi^6} + \frac{\langle \bar{q}g\sigma Gq \rangle s_0^5}{368640\pi^6} \quad (39)$$

Once again the masses are obtained dividing (37) by (36) and (39) by (38). The results are shown in figure 8.

The figure shows clearly that both currents give the same results in this approximation of the OPE, and both are below the candidate mass. It should be noted that this result may change a lot for  $\eta_I^\Xi$  if we add higher dimension condensates. In this approximation both contributions had the same polynomial in  $t$  ( $c_1$ ) thus eliminating the dependence in  $t$ . This coincidence will hardly be repeated in higher dimensions.

To summarize: we have found that due to the slow convergence of the OPE and to the relative importance of the QCD continuum contribution into the spectral function, the minimal duality ansatz “one resonance + QCD continuum” is not sufficient for finding a *sum rule window* where the results are optimal. These features penalize *all* existing sum rule results in the literature, which then become unreliable despite the fact that the mass predictions reproduce quite well the expected number.



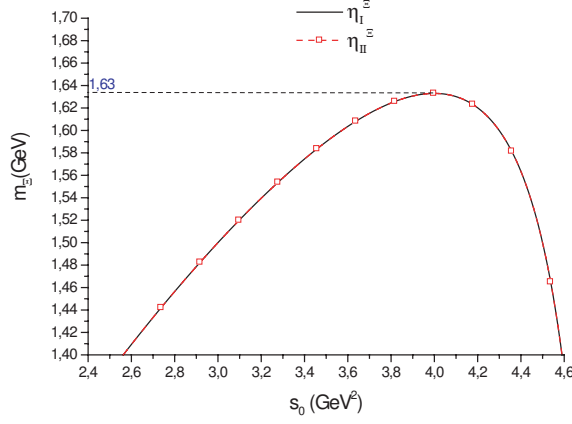


FIG. 8:  $m_{\Xi}$  obtained with the FESR up to dimension 5 condensates. The values at the stability regions are indicated on the left.

## VI. $\Theta$ DECAY

We turn now to the pentaquark decay  $\Theta \rightarrow nK^+$ . One of the most puzzling characteristics of the pentaquark is its extremely small width (much) below 10 MeV which poses a serious challenge to all theoretical models. Many explanations for this narrow width have been advanced [3]. In this section we review the calculation of the  $\Theta$  decay with QCDSR.

As we have seen in the preceding sections, a common problem of all QCDSR pentaquark mass determinations is the large continuum contribution which has its origin in the high dimension of the interpolating currents and results in a strong dependence on the continuum threshold. Another problem is the irregular behavior of the operator product expansion (OPE), which is dominated by higher dimension operators and not by the perturbative term as it should be.

Here we review the sum rule determination [22] for the decay width based on a three-point function for the decay  $\Theta \rightarrow nK^+$ . In this way it is possible to extract the coupling  $g_{\Theta nK}$ , which is directly related to the pentaquark width. The pentaquark is treated as a diquark-diquark-antiquark with one scalar and one pseudoscalar diquark in a relative S-wave.

In [19, 31] it has been argued that such a small decay width can only be explained if the pentaquark is a genuine 5-quark state, i.e., it contains no color singlet meson-baryon contributions and thus color exchange is necessary for the decay. The analysis presented both in [19] and in [31] is only qualitative. The narrowness of the pentaquark width can then be attributed to the non-trivial color structure of the pentaquark which requires the exchange of, at least, one gluon. In [22] we have done a quantitative test of the conjecture advanced in [19] and [31].

### A. The three-point functions

The investigation of the pentaquark decay width requires a three-point function which we define as

$$\Gamma(p, p') = \int d^4x d^4y e^{-iqy} e^{ip'x} \Gamma(x, y),$$

$$\Gamma(x, y) = \langle 0 | T \{ \eta_N(x) j_K(y) \bar{\eta}_\Theta(0) \} | 0 \rangle, \quad (40)$$

where  $\eta_N$ ,  $j_K$  and  $\eta_\Theta$  are the interpolating fields associated with neutron, kaon and  $\Theta$ , respectively [22].

We next consider the expression (40) in terms of hadronic degrees of freedom and write the phenomenological side of the sum rule. Treating the kaon as a pseudoscalar particle, the interaction between the three hadrons is described by the following Lagrangian density:

$$\begin{aligned} \mathcal{L} &= ig_{\Theta nK} \bar{\Theta} \gamma_5 K n \quad \text{for } P = + \\ \mathcal{L} &= ig_{\Theta nK} \bar{\Theta} K n \quad \text{for } P = - \end{aligned} \quad (41)$$

Writing the correlation function (40) in momentum space and inserting complete sets of hadronic states we obtain an expression which depends on the following matrix elements:

$$\begin{aligned} -iV(p, p') &= \langle n(p', s') | \Theta(p, s) K(q) \rangle, \\ \langle 0 | \eta_N | n(p', s') \rangle &= \lambda_N u^s(p'), \\ \langle K(q) | j_K | 0 \rangle &= \lambda_K, \\ \langle \Theta(p, s) | \bar{\eta}_\Theta | 0 \rangle &= \lambda_\Theta \bar{u}^s(p) \quad \text{for } P = + \\ \langle \Theta(p, s) | \bar{\eta}_\Theta | 0 \rangle &= -\lambda_\Theta \bar{u}^s(p) \gamma_5 \quad \text{for } P = - \end{aligned} \quad (42)$$

Using the simple Feynman rules derived from (41) we can rewrite  $V(p, p')$  as

$$\begin{aligned} V(p, p') &= -g_{\Theta nK} \bar{u}^s(p') \gamma_5 u^s(p) \quad P = + \\ V(p, p') &= -g_{\Theta nK} \bar{u}^s(p') u^s(p) \quad P = - \end{aligned} \quad (43)$$

The coupling constants  $\lambda_N$  and  $\lambda_\Theta$  can be determined from the QCD sum rules of the corresponding two-point functions.  $\lambda_K$  is related to the kaon decay constant through

$$\lambda_K = \frac{f_K m_K^2}{m_u + m_s}. \quad (44)$$

Combining the expressions above we arrive at

$$\begin{aligned} \Gamma_{phen} &= \frac{-g_{\Theta nK} \lambda_\Theta \lambda_N \lambda_K}{(p'^2 - m_N^2)(q^2 - m_K^2)(p^2 - m_\Theta^2)} \\ &\times \Gamma_E + \text{continuum} \end{aligned} \quad (45)$$

with

$$\begin{aligned} \Gamma_E &= \sigma^{\mu\nu} \gamma_5 q_\mu p'_\nu - im_N \not{q} \gamma_5 \\ &+ i(m_N \mp m_\Theta) \not{p}' \gamma_5 \\ &+ i\gamma_5 (p'^2 \mp m_\Theta m_N - qp') \end{aligned} \quad (46)$$

We have worked with the  $\sigma^{\mu\nu} \gamma_5 q_\mu p'_\nu$  structure because, as it was shown in [34], this structure gives results which are

less sensitive to the coupling scheme on the phenomenological side, i.e., to the choice of a pseudoscalar or pseudovector coupling between the kaon and the baryons.

Coming back to (40) we write the interpolating fields in terms of quark degrees of freedom as

$$\begin{aligned} j_K(y) &= \bar{s}(y)i\gamma_5 u(y), \\ \eta_N(x) &= \epsilon^{abc}(d_a^T(x)C\gamma_\mu d_b(x))\gamma_5\gamma^\mu u_c(x), \\ \bar{\eta}_\Theta(0) &= -\epsilon^{abc}\epsilon^{def}\epsilon^{cfg}s_g^T(0)C \\ &\quad \times [\bar{d}_e(0)\gamma_5 C\bar{u}_d^T(0)][\bar{d}_b(0)C\bar{u}_a^T(0)]. \end{aligned} \quad (47)$$

The pentaquark current above (proposed in [16]) contains a pseudoscalar and a scalar diquark. With these diquarks the two point function might receive a significant contribution from instantons. In [35] we have studied a situation in which these instanton contributions affected the two-point function but gave a negligible contribution to the three-point function. Moreover, in [36] we have observed that instantons give a negligible contribution to heavy baryon weak decays. Motivated by these results, in this first calculation we have neglected instantons.

Inserting the currents into (40), the resulting expression involves the quark propagator in the presence of quark and gluon condensates (13). Using it we arrive at a final complicated expression for the correlator, which is represented schematically by the sum of the diagrams of Fig. 9.

Let us consider the phenomenological side (45) and, following [37], rewrite it generically as:

$$\Gamma(q^2, p^2, p'^2) = \Gamma_{pp} + \Gamma_{pc1} + \Gamma_{pc2} + \Gamma_{cc} \quad (48)$$

where  $\Gamma_{pp}(q^2, p^2, p'^2)$  stands for the pole-pole part and reads

$$\Gamma_{pp} = \frac{-g_{\Theta nK} \lll}{(p^2 - m_\Theta^2)(p'^2 - m_N^2)(q^2 - m_K^2)} \quad (49)$$

The continuum-continuum term  $\Gamma_{cc}$  can be obtained as usual, with the assumption of quark-hadron duality [22].

The pole-continuum transition terms are contained in  $\Gamma_{pc1}$  and  $\Gamma_{pc2}$ . They can be explicitly written as a double dispersion integral:

$$\begin{aligned} \Gamma_{pc1} &= \int_{m_{K^*}^2}^{\infty} \frac{b_1(u, p^2) du}{(m_N^2 - p'^2)(u - q^2)}, \\ \Gamma_{pc2} &= \int_{m_{N^*}^2}^{\infty} \frac{b_2(s, p^2) ds}{(m_K^2 - q^2)(s - p'^2)}. \end{aligned} \quad (50)$$

Since there is no theoretical tool to calculate the unknown functions  $b_1(u, p^2)$  and  $b_2(s, p^2)$  explicitly, one has to employ a parametrization for these terms. We will use two different parametrizations: one with a continuous function for the  $\Theta$  and one where the pole term is singled out.

We assume here that the functions  $b_1$  and  $b_2$  have the following form:

$$\begin{aligned} b_1(u, p^2) &= \tilde{b}_1(u) \int_{m_\Theta^2}^{\infty} d\omega \frac{b_1(\omega)}{\omega - p^2} \\ b_2(s, p^2) &= \tilde{b}_2(s) \int_{m_\Theta^2}^{\infty} d\omega \frac{b_2(\omega)}{\omega - p^2} \end{aligned} \quad (51)$$

with continuous functions  $b_{1,2}(w)$ , starting from  $m_\Theta^2$ . This is our **parametrization A**. The functions  $\tilde{b}_1(u)$  and  $\tilde{b}_2(s)$  describe the excitation spectra of the kaon and the nucleon, respectively. After Borel transform, the pole-continuum term contains one unknown constant factor which can be determined from the sum rules.

In order to investigate the role played by the  $\Theta$  continuum, we explicitly force the phenomenological side to contain only the pole part of the  $\Theta$ , both in the pole-pole term and in the pole-continuum terms. This can formally be done by choosing  $b_1(\omega) = b_2(\omega) = \delta(\omega - m_\Theta^2)$  in (51) and the functions then read:

$$\begin{aligned} b_1(u, p^2) &= \frac{\tilde{b}_1(u)}{m_\Theta^2 - p^2}, \\ b_2(s, p^2) &= \frac{\tilde{b}_2(s)}{m_\Theta^2 - p^2}. \end{aligned} \quad (52)$$

This is our **parametrization B**. In this case we have the  $\Theta$  in the ground state. Again, in the final expressions this gives additional constants which can be calculated.

## B. Decay sum rules

The sum rule may be written identifying the phenomenological and theoretical descriptions of the correlation function. As mentioned above, we work with the  $\sigma^{\mu\nu}\gamma_5 q_\mu p'_\nu$  structure. In the case of the three-point function considered here, there are two independent momenta and we may perform either a single or a double Borel transform. We first consider the choice:

$$(I) \quad q^2 = 0 \quad p^2 = p'^2 \quad (53)$$

and perform a single Borel transform:  $p^2 = -P^2$  and  $P^2 \rightarrow M^2$ . In this case we take  $m_K^2 \simeq 0$  and single out the  $1/q^2$ -terms. The second choice is:

$$(II) \quad q^2 \neq 0 \quad p^2 = p'^2. \quad (54)$$

Here we perform two Borel transforms:  $p^2 = -P^2$  and  $P^2 \rightarrow M^2$  and also  $q^2 = -Q^2$  and  $Q^2 \rightarrow M'^2$ . We have also considered the choice  $q^2 = p^2 = p'^2 = -P^2$ , performing one single Borel transform ( $P^2 \rightarrow M^2$ ). However, we were not able to find a stable sum rule. Introducing the notation  $G = -g_{\Theta nK}\lambda_\Theta\lambda_N\lambda_K$  and using (I) and (II) we obtain the following sum rules:

### Method I:

$$\Gamma_{pp}(M^2) + \Gamma_{pc2}(M^2) = \int_0^{s_0} ds \rho_{th}(s) e^{-s/M^2} \quad (55)$$

with

$$\Gamma_{pp}(M^2) = G \frac{e^{-m_\Theta^2/M^2} - e^{-m_N^2/M^2}}{m_\Theta^2 - m_N^2} \quad (56)$$

and for the pole-continuum part we obtain

$$\begin{aligned}\Gamma_{pc2}(M^2) &= A e^{-m_{N^*}^2/M^2} \quad \text{param. A} \\ \Gamma_{pc2}(M^2) &= A e^{-m_{\Theta}^2/M^2} \quad \text{param. B}\end{aligned}\quad (57)$$

In both parametrizations the term  $\Gamma_{pc1}$  is exponentially suppressed and, as discussed in [37], has been neglected.  $A$  is an unknown constant and can be determined from the sum rules.

### Method II

$$\Gamma_{pp}(M^2, M'^2) + \Gamma_{pc2}(M^2, M'^2) = \quad (58)$$

$$\int_0^{u_0} du \int_0^{s_0} ds \rho_{th}(s, u) e^{-s/M^2} e^{-u/M'^2} \quad (59)$$

with

$$\Gamma_{pp} = G e^{-m_K^2/M'^2} \frac{e^{-m_{\Theta}^2/M^2} - e^{-m_N^2/M^2}}{m_{\Theta}^2 - m_N^2} \quad (60)$$

and with

$$\Gamma_{pc2} = A e^{-m_K^2/M'^2} e^{-m_{N^*}^2/M^2} \quad (61)$$

for parametrization A and

$$\Gamma_{pc2} = A e^{-m_K^2/M'^2} e^{-m_{\Theta}^2/M^2} \quad (62)$$

for parametrization B. Also in this case  $\Gamma_{pc1}$  is exponentially suppressed. In the above expressions  $\rho_{th}$  is the double discontinuity computed directly from the theoretical (OPE) description of the correlation function (see [22] for details and also [38]) and  $s_0$  is the continuum threshold of the nucleon defined as  $s_0 = (m_N + \Delta_N)^2$ .

### C. Decay width

The hadronic masses are  $m_N = 938$  MeV,  $m_{N^*} = 1440$  MeV,  $m_K = 493$  MeV and  $m_{\Theta} = 1540$  MeV. For each of the sum rules above (Eqs. (55) and (58)) we can take the derivative with respect to  $1/M^2$  and in this way obtain a second sum rule. In each case we have thus a system of two equations and two unknowns ( $G$  and  $A$ ) which can then be easily solved.

The couplings constants  $\lambda_N$  and  $\lambda_{\Theta}$  are taken from the corresponding two-point functions:

$$\lambda_N = (2.4 \pm 0.2) \times 10^{-2} \text{ GeV}^3 \quad (63)$$

$$\lambda_{\Theta} = (2.4 \pm 0.3) \times 10^{-5} \text{ GeV}^6 \quad (64)$$

The coupling  $\lambda_K$  is obtained from (44) with  $f_K = 160$  MeV,  $m_s = 100$  MeV and  $m_u = 5$  MeV:

$$\lambda_K = 0.37 \text{ GeV}^2. \quad (65)$$

In Fig. 9, among these OPE diagrams there are two distinct subsets. In the first two lines of the figure there is no

gluon line connecting the “petals” and therefore no color exchange. A diagram of this type we call color-disconnected. In the second subset of diagrams, in the third line of the figure, we have color exchange. If there is no color exchange, the final state containing two color singlets was already present in the initial state, before the decay, as noticed in [20]. In this case the pentaquark had a component similar to a  $K - n$  molecule. In the second case the pentaquark was a genuine 5-quark state with a non-trivial color structure. We may call this type of diagram a color-connected (CC) one. In our analysis we write sum rules for both cases: all diagrams and only color-connected. The former case is standard in QCDSR calculations and therefore we omit details and present only the results. The latter case implies that the pentaquark is a genuine 5-quark state and the evaluation of  $g_{\Theta n K}$  is thus based only on the CC diagrams. We work in the Borel window given by  $1 \text{ GeV}^2 \leq M^2(M'^2) \leq 1.5 \text{ GeV}^2$ . Since the strange mass is small, the dominating diagram is Fig. 9b of dimension three with one quark condensate. In the range considered, the dimension 5 condensates are substantially suppressed compared to this term.

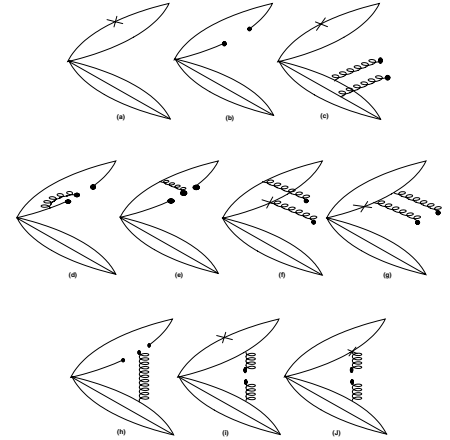


FIG. 9: The main diagrams which contribute to the theoretical side of the sum rule in the relevant structure. a) - g) are the color-disconnected diagrams, whereas h) - j) are the color-connected diagrams. The cross indicates the insertion of the strange mass.

We have found out that the contribution from the pole-continuum part is of a similar size as the pole part. For lower values of  $M^2$  around  $1 \text{ GeV}^2$ , the pole contribution dominates, however, for larger values of  $M^2$  the importance of the pole-continuum contribution grows and eventually becomes larger than the pole part. This is an additional reason to restrict the analysis to small values for the Borel parameters.

We have evaluated the sum rules for the coupling constant computed with all diagrams of Fig. 9 and we have found that they are very stable. We give the values of the coupling extracted at  $M^2 = 1.5 \text{ GeV}^2$  and  $M'^2 = 1 \text{ GeV}^2$  in Table I. We present our results for the coupling constant  $g_{\Theta n K}$  obtained with the color connected diagrams only. In Fig. 10 we show the coupling, given by the solution of the sum rule I A (55), as a function of the Borel mass squared  $M^2$ . Different lines show

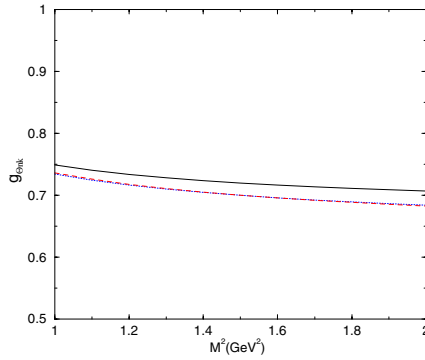


FIG. 10:  $|g_{\Theta nK}|$  in case I A with three different continuum threshold parameters. Solid line:  $\Delta_N = 0.5$  GeV, dotted line:  $\Delta_N = 0.4$  GeV, dash-dotted line:  $\Delta_N = 0.6$  GeV.

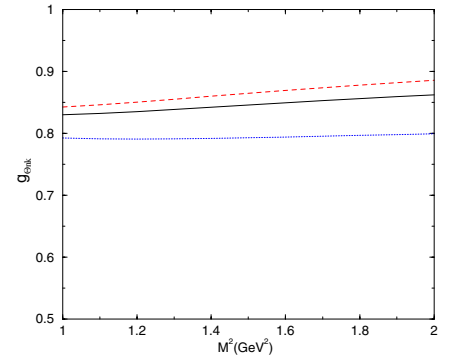


FIG. 12:  $|g_{\Theta nK}|$  in case I B with three different continuum threshold parameters. Solid line:  $\Delta_N = 0.5$  GeV, dotted line:  $\Delta_N = 0.4$  GeV, dash-dotted line:  $\Delta_N = 0.6$  GeV.

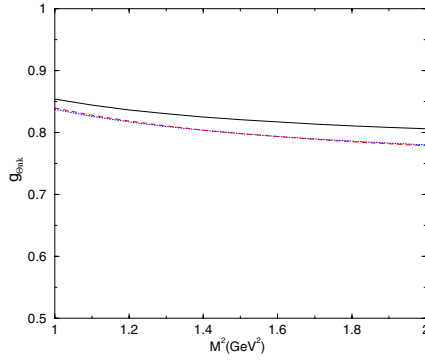


FIG. 11:  $|g_{\Theta nK}|$  in case II A. Solid line:  $\Delta_N = 0.5$  GeV. Dotted line:  $\Delta_N = 0.4$  GeV. Dashed line:  $\Delta_N = 0.6$  GeV.  $M'^2 = 1$  GeV<sup>2</sup>.

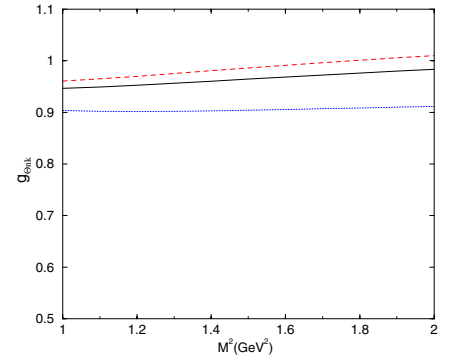


FIG. 13:  $|g_{\Theta nK}|$  in case II B. Solid line:  $\Delta_N = 0.5$  GeV. Dotted line:  $\Delta_N = 0.4$  GeV. Dashed line:  $\Delta_N = 0.6$  GeV.  $M'^2 = 1$  GeV<sup>2</sup>.

different values of the continuum threshold  $\Delta_N$ . As it can be seen,  $g_{\Theta nK}$  is remarkably stable with respect to variations both in  $M^2$  and in  $\Delta_N$ . In Fig. 11 we show the coupling obtained with the sum rule II A (58). We find again fairly stable results which are very weakly dependent on the continuum threshold. In Fig. 12 we show the results of the sum rule I B. In Fig. 13 we present the result of the sum rule II B. The meaning of the different lines is the same as in the previous figures. The results are similar to the cases before.

TABLE I: Table I:  $g_{\Theta nK}$  for various cases  $g_{\Theta nK}$  for various cases

case	$ g_{\Theta nK} $ (CC)	$ g_{\Theta nK} $ (all diagrams)
I A	0.71	2.59
II A	0.82	3.59
I B	0.84	3.24
II B	0.96	4.48

In Table I we present a summary of our results for  $g_{\Theta nK}$  giving emphasis to the difference between the results obtained with all diagrams and with only the color-connected ones. For the continuum thresholds we have employed  $\Delta_N = \Delta_K = 0.5$  GeV.

For our final value of  $g_{\Theta nK}$  we take an average of the sum rules I A - II B. It is interesting to observe that the influence of the continuum threshold is relatively small, especially when compared to the corresponding two-point functions.

Considering the uncertainties in the continuum thresholds, in the coupling constants  $\lambda_{K,N,\Theta}$  and in the quark condensate we get an uncertainty of about 50%. Our final result then reads:

$$|g_{\Theta nK}|(\text{all diagrams}) = 3.48 \pm 1.8, \\ |g_{\Theta nK}|(\text{CC}) = 0.83 \pm 0.42. \quad (66)$$

Including all diagrams, the prediction for  $\Gamma_{\Theta}$  is then 13 MeV (652 MeV) for a positive (negative) parity pentaquark. In the CC case we get a width of 0.75 MeV (37 MeV) for a positive (negative) parity pentaquark. The measured upper limit of the width is around 5-10 MeV both in the Kn channel (considered

here) and in the  $K\rho$  channel.

To summarize: we have presented a QCD sum rule study of the decay of the  $\Theta^+$  pentaquark using a diquark-diquark-antiquark scheme with one scalar and one pseudoscalar diquark. Based on the evaluation of the relevant three-point function, we have computed the coupling constant  $g_{\Theta nK}$ . In the operator product expansion we have included all diagrams up to dimension 5. In this particular type of sum rule a complication arises from the pole-continuum transitions which are not exponentially suppressed after Borel transformation and must be explicitly included. The analysis was made for two different pole-continuum parametrizations and in two different evaluation schemes. The results are consistent with each other. In addition, we have tested the ideas presented in [19, 31] by including only diagrams with color exchange. Our final results are given in eq. (66). We conclude that for a positive parity pentaquark a width much smaller than 10 MeV would indicate a pentaquark which contains no color-singlet meson-baryon contribution. For a negative parity pentaquark, even under the assumption that it is a genuine 5-quark state, we could not explain the narrow width of the  $\Theta$ .

## VII. CONCLUSION

In this review we have discussed only our works on pentaquarks in a somewhat critical perspective. Most of the other calculations, most of them quoted here, have the same successes and difficulties as ours. Looking back and taking distance, we might say that the work done over the last two years has undergone continuous improvements in quality. At the very beginning, in the heat of the discovery hours, some works were done in rush and with a certain negligence in various aspects. For example, in the very first paper [14] reproducing the  $\Theta$  mass, no analysis of the OPE convergence was presented and neither an estimate of the continuum contribution was performed. The second round of calculations went much deeper in the details of QCDSR procedures. However it was not just a matter of “doing better” what we already knew how to do. The method had to face new challenges. For example:

in the pentaquark study, for the first time, we were dealing with a system that could be composed by independent sub-systems, like two non-interacting hadrons. In [20] this configuration was dubbed “two-hadron reducible” component. It has been a subject of debate how to disentangle and subtract this component from the final results. Also, the more quarks we have, the less unique is the definition of the interpolating current. Increasing the number of lines introduces new technical complications for the evaluation of the OPE. The efforts of the community to overcome all these problems were very productive. All in all, we can say that pentaquarks have done more for QCDSR than these have done for pentaquarks.

To conclude we come back to the question raised in the introduction: “How could we calculate the correct mass of something that does not exist?” In the light of the discussion presented in the last sections, a sober answer would be: although we started reproducing unfounded experimental results, it was just a matter of time until we would reach a situation where, reproducing these data would be so artificial as it was to use the notion of “aether” in the years of the birth of special relativity. At some point we would be obliged to push and twist the method so far, that some more audacious groups would be brave enough to go against the “experimental evidence” and put doubts on the experiments. This attitude was already taken by some phenomenologists [7, 39], by some experimentalists [40] and by lattice theorists.

The final feeling is that all this work was fruitful and there is nothing to be regretted.

## VIII. ACKNOWLEDGEMENTS

We are grateful to FAPESP and to CNPq for financial support. Discussions with Markus Eidemüller, Rômulo Rodrigues da Silva and Stephan Narison are gratefully acknowledged.

- 
- [1] T. Nakano *et al.*, LEPS Coll., Phys. Rev. Lett. **91**, 012002 (2003).
  - [2] F. Close, Nature **435**, 287 (2005); M. Ostrick, Prog. Part. Nucl. Phys. **55**, 337 (2005); D. Barna, Acta Phys. Hung. A **22**, 187 (2005); M. Danilov, hep-ex/0509012. K. Hicks, AIP Conf. Proc. **756**, 195 (2005).
  - [3] For recent reviews see: M. Karliner, Int. J. Mod. Phys. A **20**, 199 (2005); Shi-Lin Zhu, Int. J. Mod. Phys. A **20**, 1548 (2005); M. Oka, J. Sugiyama, and T. Doi, Nucl. Phys. A **755**, 391 (2005); A. Hosaka, hep-ph/0506138; S. H. Lee, H. Kim, and Y. s. Oh, J. Korean Phys. Soc. **46**, 774 (2005).
  - [4] M. Battaglieri, R. De Vita, and V. Kubarovsky [CLAS Collaboration], AIP Conf. Proc. **806**, 48 (2006).
  - [5] M. Battaglieri, R. De Vita, V. Kubarovsky, and P. Stoler [CLAS Collaboration], JLAB-PHY-06-09 *Contributed to 25th International Symposium on Physics in Collision (PIC 05), Prague, Czech Republic, 6-9 Jul 2005*
  - [6] T. Barnes, hep-ph/0510365.
  - [7] A. R. Dzierba, C. A. Meyer, and A. P. Szczepaniak, J. Phys. Conf. Ser. **9**, 192 (2005). hep-ex/0412077.
  - [8] F. Csikor, Z. Fodor, S. D. Katz, and T. G. Kovacs, Int. J. Mod. Phys. A **20**, 4562 (2005) and references therein.
  - [9] F. Csikor *et al.*, JHEP **0311**, 70 (2003); T.W. Shiu, T.H. Hsieh, hep-ph/0403020; N. Matur *et al.*, hep-ph/0406196.
  - [10] S. Sasaki, hep-lat/0310014.
  - [11] For a review and references to original works, see e.g., S. Narison, *QCD as a theory of hadrons*, Cambridge Monogr. Part. Phys. Nucl. Phys. Cosmol. **17**, 1 (2002); *QCD spectral sum rules*, World Sci. Lect. Notes Phys. **26**, 1 (1989); Acta Phys. Pol. **26**, 687 (1995); Riv. Nuov. Cim. **10N2**, 1 (1987); Phys. Rep. **84**, 1 (1982).
  - [12] M.A. Shifman, A.I. Vainshtein, and V.I. Zakharov, Nucl. Phys.

- B147, 385 (1979).
- [13] L.J. Reinders, H. Rubinstein, and S. Yazaki, Phys. Rep. **127**, 1 (1985).
  - [14] S.-L. Zhu, Phys. Rev. Lett. **91**, 232002 (2003).
  - [15] R.D. Matheus, F.S. Navarra, M. Nielsen, R. Rodrigues da Silva, and S.H. Lee, Phys. Lett. B **578**, 323 (2004).
  - [16] J. Sugiyama, T. Doi, and M. Oka, Phys. Lett. B **581**, 167 (2004).
  - [17] M. Eidemüller, Phys. Lett. B **597**, 314 (2004).
  - [18] R.D. Matheus, F.S. Navarra, M. Nielsen, and R. Rodrigues da Silva, Phys. Lett. B **602**, 185 (2004).
  - [19] R.D. Matheus, S. Narison, hep-ph/0412063.
  - [20] Y. Kondo, O. Morimatsu, and T. Nishikawa, Phys. Lett. B **611**, 93 (2005); Y. Kwon, A. Hosaka, and S. H. Lee, hep-ph/0505040.
  - [21] Hungchong Kim, Su Houn Lee, Phys. Lett. B **595**, 293 (2004).
  - [22] M. Eidemüller, F. S. Navarra, M. Nielsen, and R. Rodrigues da Silva, Phys. Rev. D **72**, 034003 (2005).
  - [23] D. Strottman, Phys. Rev. D **20**, 748 (1979).
  - [24] This configuration was considered in the case of a  $uudc\bar{c}$  state in: S.J. Brodsky, I. Schmidt, and G. F. de Teramond, Phys. Rev. Lett. **64**, 1011 (1990).
  - [25] M. Karliner and H. Lipkin, hep-ph/0307243.
  - [26] R. Jaffe and F. Wilczek, Phys. Rev. Lett. **91**, 232003 (2003).
  - [27] E. Shuryak and I. Zahed, Phys. Lett. B **589**, 21 (2004).
  - [28] B. L. Ioffe, Nucl. Phys. B **188**, 317 (1981); B **191**, 591(E) (1981).
  - [29] Y. Chung, H. G. Dosch, M. Kremer, and D. Schall, Phys. Lett. B **102**, 175 (1981); Nucl. Phys. B **197**, 55 (1982).
  - [30] K.-C. Yang *et al.*, Phys. Rev. D **47**, 3001 (1993).
  - [31] B. L. Ioffe and A. G. Oganesian, JETP Lett. **80**, 386 (2004); A. G. Oganesian, hep-ph/0410335.
  - [32] R. A. Bertlmann, C.A. Dominguez, G. Launer, and E. de Rafael, Nucl. Phys. B **250**, 61 (1985); R. A. Bertlmann, G. Launer, and E. de Rafael, Z. Phys. C **39**, 231 (1988).
  - [33] K. Chetyrkin, N.V. Krasnikov, and A.N. Tavkhelidze, Phys. Lett. B **76**, 83 (1978); N.V. Krasnikov, A.A. Pivovarov, and A.N. Tavkhelidze, Z. Phys. C **19**, 301 (1983).
  - [34] H. Kim, S.H. Lee, and M. Oka, Phys. Lett. B **453**, 199 (1999); Phys. Rev. D **60**, 034007 (1999); M.E. Bracco, F.S. Navarra, and M. Nielsen, Phys. Lett. B **454**, 346 (1999).
  - [35] H. G. Dosch, E. M. Ferreira, F. S. Navarra, and M. Nielsen, Phys. Rev. D **65**, 114002 (2002).
  - [36] R. S. Marques de Carvalho, F. S. Navarra, M. Nielsen, E. Ferreira, and H. G. Dosch, Phys. Rev. D **60**, 034009 (1999).
  - [37] B. Ioffe and A. Smilga, Nucl. Phys. B **232**, 109 (1984).
  - [38] M. E. Bracco, M. Chiapparini, A. Lozea, F. S. Navarra, and M. Nielsen, Phys. Lett. B **521**, 1 (2001).
  - [39] J. Haidenbauer and G. Krein, Phys. Rev. C **68**, 052201 (2003).
  - [40] H. G. Fischer and S. Wenig, Eur. Phys. J. C **37**, 133 (2004).